Published in final edited form as:
Exp Cell Res. 2007 October 1; 313(16): 3542–3555. doi:10.1016/j.yexcr.2007.07.011.

CENTRAL ROLE OF α9 ACETYLCHOLINE RECEPTOR IN COORDINATING KERATINOCYTE ADHESION AND MOTILITY AT THE INITIATION OF EPITHELIALIZATION

Alex I. Chernyavsky, **Juan Arredondo**, **Douglas E. Vetter***, and **Sergei A. Grando**
Departments of Dermatology, University of California, Irvine, CA

* *Department of Neuroscience, Tufts University School of Medicine, Boston, MA, USA*

Abstract

Epithelialization, a major component of wound healing, depends on keratinocyte adhesion and migration. Initiation of migration relies upon the ability of keratinocytes to free themselves from neighboring cells and basement membrane. The local cytotransmitter acetylcholine (**ACh**) controls keratinocyte adhesion and locomotion through different classes of ACh receptors (**AChR**). In this study, we explored signaling pathways downstream of the α9 AChR subtype that had been shown to control cell shape and cytoplasm mobility. Inactivation of α9 signaling by pharmacologic antagonism and RNA interference in keratinocyte cultures and null mutation in knockout mice delayed wound re-epithelization in vitro and in vivo, respectively, and diminished the extent of colony scattering and cell outgrowth from the megacolony. Although keratinocytes at the leading edge elongated, produced filopodia and moved out, most of them remained anchored to the substrate by long cytoplasmic processes that stretched during their migration instead of retracting the uropod. Since the velocity of keratinocyte migration was not altered, we investigated the role of α9 in assembly/disassembly of the cell-cell and cell-matrix adhesion complexes. Stimulation of α9 upregulated in a time-dependent fashion phosphorylation of the adhesion molecules comprising focal adhesions (FAK, paxillin) and intercellular junctions (β-catenin, desmoglein 3) as well as cytokeratins. Stimulation of α9 was associated with activation of phospholipase C, Src, EGF receptor kinase, protein kinase C, Rac and Rho, whereas inhibition of this receptor interfered with phosphorylation of adhesion and cytoskeletal proteins, and also altered cell-cell cohesion. We conclude that signaling through α9 AChR is critical for completion of the very early stages of epithelialization. By activating α9 AChR, ACh can control the dynamics and strength of cell-cell cohesion, disabling of a trailing uropod and disassembly and re-assembly of focal adhesions, thus facilitating crawling locomotion.

Keywords

keratinocytes; wound epithelialization; cell matrix adhesion; cell-cell adhesion; migration; phosphorylation

Correspondence to: Sergei A. Grando, MD, PhD, DSc, Department of Dermatology, University of California Irvine, C340 Medical Sciences I, Irvine, CA 92697, USA, Phone 949-824-2713, Fax: 949-824-2993, e-mail: E-mail: sgrando@uci.edu.

INTRODUCTION

Epithelialization—a major component of wound healing—relies not only on proliferation, but also on detachment, lateral migration (crawling locomotion) and re-attachment of epidermal keratinocytes (**KCs**) (reviewed in [1]). The launching of lateral migration depends upon the ability of KCs to free themselves from neighboring cells and basement membrane. Keratinocyte crawling locomotion involves cyclic changes in local adhesive strength regulated by a variety of inter- and intracellular signals. When cell collisions prevent further migration, cell-cell attachment occurs. The newly immobilized KCs form desmosomes that link them together. The regulatory mechanisms allowing KCs to disassemble and reassemble their cell-matrix and cell-cell attachments are the subject of intense research. Although functional components of adhesion complexes are well known, much less is known about the signaling mechanisms that initiate, sustain and terminate adhesion. The purpose of this research was to elucidate autocrine/paracrine signaling pathways mediating biochemical and phenotypic alterations of KCs during the earliest stages of epithelialization.

Keratinocyte adhesion is mediated primarily by four structures: hemidesmosomes and focal adhesions, which function in cell-matrix adhesion, and desmosomes and adherens junctions, which function in cell-cell adhesion (reviewed in [2]). Focal adhesions are the points at which crawling KCs make their closest contacts with a substrate. They provide the primary stabilizing force for leading lamella and serve as an abutment during forward relocation of the cell body. As the cell body advances, the focal adhesion sites move backward in relation to the direction of cell movement and form a trailing uropod. Adherens junctions are assembled by classical cadherins that form homodimers with other cadherin molecules on adjacent cells and interact with the submembrane catenins linked to the actin cytoskeleton. Desmosomal junctions are comprised of the core protein families of desmogleins and desmocollins, which form both homo-and heterotypic interactions extracellularly, and tether keratin intermediate filaments to the plasma membrane intracellularly. Phosphorylation and dephosphorylation of components of adhesion complexes are probably the most important regulatory events altering both their structural integrity and adhesive capacity. The network underlying phosphorylation of adhesion molecules is rather complex and interdependent with pathways mediating cell response to various kinds of environmental stimuli downstream of growth factor receptors, G-protein coupled receptors, and ion channels/pumps. Some intercellular junction proteins are phosphorylated on serine, some on tyrosine and some on both residues, leading to diverse effects on the adhesive properties of these molecules.

The local cytotransmitter acetylcholine (**ACh**), endogenously produced and secreted by KCs, controls keratinocyte adhesion and locomotion through different classes of ACh receptors (**AChRs**) (reviewed in [3]). There is an upward concentration gradient of free ACh in human epidermis, and the repertoire of cholinergic enzymes and receptors changes with cell maturation, so that at each stage of their development, KCs respond to ACh *via* different combinations of nicotinic and muscarinic classes of AChRs. ACh is essential for maintenance of the polygonal cell shape and intercellular junctions by KCs, and individual subtypes of AChRs produce distinct effects on cell adhesive function. The α9 subunit is a distant member of the nicotinic AChR gene family and can form Ca^{2+}-permeable ACh-gated ion channels [4]. It is the first known representative of a novel class of cholinergic receptors with dual, muscarinic and nicotinic pharmacology and ionotropic functions coupled to regulation of intracellular Ca^{2+} metabolism [4,5]. α9 also can assemble with α10 to form a heteropentameric channel with similar pharmacologic properties [6]. Co-assembly, however, modifies the physiological response to ACh compared to α9 homomers, most notably with respect to receptor desensitization. Previous studies revealed an important role of α9 AChR in regulation of cell shape, cytoplasm mobility and intercellular cohesion of KCs (reviewed in [7]).

In this study, we investigated the role of α9 AChR in initiation of keratinocyte migration. Inactivation of α9 signaling delayed wound epithelization *in vitro* and *in vivo*, and diminished the ability of individual KCs to detach from culture substrate. Stimulation of α9 upregulated, in a time-dependent fashion, phosphorylation of the adhesion molecules comprising focal adhesions, adherens and desmosomal junctions, and cytokeratins. The components of the signaling cascade included Src, epidermal growth factor receptor (**EGFR**) kinase, phospholipase C (**PLC**), protein kinase C (**PKC**), as well as the small GTPases Rho and Rac. Thus, signaling through α9 AChR was found to be critical for completion of the early stages of wound epithelialization. By activating α9 AChRs, ACh can control the dynamics and strength of cell-matrix and cell-cell attachments and disabling of trailing uropod. These findings unveil a novel biologic mechanism of cholinergic regulation of epithelial cell motility that has salient clinical implications for maintaining the integrity of the mucocutaneous barrier, and prevention of cancer metastases.

MATERIALS AND METHODS

Chemicals and tissue culture reagents

ACh, the α9-preferring agonist methylcarbachol (**MCC**) [8] and the antagonists 3-tropanyl-indole-3-carboxylate hydrochloride (ICS-205-930; **ICS)** and strychnine (**Str**) [9,10], the metabolic inhibitor of ACh synthesis hemicholinium-3 (**HC-3**) [11,12], heat-inactivated newborn calf serum, Wright's stain and all secondary antibodies were purchased from Sigma-Aldrich Corporation, Inc. (St. Louis, MO). Serum-free keratinocyte growth medium (**KGM**) containing 5 ng/ml EGF and 50 μg/ml bovine pituitary extract was from GIBCO-BRL (Cambridge, MA). Agarose type A was obtained from Accurate Chemical & Scientific Corporation (Westbury, NY). Human recombinant EGF and hepatocyte growth factor/scatter factor (**HGF/SF**) and mouse IgG phosphoserine/threonine antibody were from BD Biosciences (San Jose, CA). Mouse monoclonal anti-human desmoglein 3 antibody was from R&D Systems, Inc. (Minneapolis, MN). Rabbit polyclonal antibodies to paxillin (phopsho Y118) and FAK (phospho Y577) were from Abcam (Cambridge, MA). Mouse monoclonal antibody to β-catenin (phospho S33) was from GeneTex, Inc. (San Antonio, TX), monoclonal antibody to pan cytokeratin was from BioLegend (San Diego, CA) and rabbit anti-α9 antibody was developed and characterized by us in the past [13]. The FACE™ c-Src and EGFR kits were purchased from Active Motif (Carlsbad CA). The Rac (STA-401) and Rho (STA-403) activation ("pull-down") assay kits were from Cell Biolabs, Inc. (San Diego, CA). The PKC activity assay kit was from Stressgen Bioreagents (Ann Arbor, MI), and the Amplex® Red phosphatidylcholine-specific PLC assay kit was from Molecular Probes (Eugene, OR). The pre-designed and tested small interfering RNA (**siRNA**) targeting human *CHRNA9* (NM_017581) mRNA (ON-TARGETplus siGENOME SMARTpool reagent M-006141-01) and negative control siRNA (**siRNA-NC**) targeting luciferase gene with the target sequence 5′-CGTACGCGGAATACTTCGA-3′ were purchased from Dharmacon (Lafayette, CO).

Cultures of human and murine KCs

Human KCs were isolated from foreskin epidermis by treating pieces of neonatal foreskins with a 0.125% trypsin solution overnight. This study has been approved by the University of California Davis Human Subjects Review Committee. The individual cells were suspended in KGM, plated in standard tissue culture flasks and cultured at 37°C in a humidified atmosphere of 5% CO_2 following the procedure detailed elsewhere [14]. The purity of cultures was investigated immunocytochemically using DAKO-CK monoclonal mouse anti-human cytokeratin antibody (MNF 116) and was consistently >95%. Murine KCs were similarly isolated from the epidermis of 1–2 d old α9+/+ and α9−/− littermates [15]. This study was approved by University of California Davis Committee on the Use of Animals in Research. Individual murine KCs were grown using the cell culture techniques optimized for mouse KCs

[16]. The purity of cultures was confirmed using anti-mouse cytokeratin antibody. Both human and murine keratinocyte cultures used in experiments were between passages 2 and 4, approximately 80% confluent, grown from at least 3 different donors. The pH of KGM containing test compounds was maintained within the range 7.2–7.4, and the osmolarity was 290–310 mOsm/kg under all experimental conditions.

Keratinocyte migration initiation assays

The effects of α9 AChR at early stages of wound epithelialization were studied using the following *in vitro* models of migration initiation. The KCs were grown to confluence at 0.09 mM Ca^{2+} in KGM containing 5 ng/ml EGF and then incubated at 1.2 mM Ca^{2+} for 6 h to allow formation of desmosomal junctions, which was confirmed by observing dotted staining pattern of desmoglein 3 at the sites of cell-cell contacts. The monolayers were then starved of EGF for 18 h. At the end of starvation, the KCs were deprived of endogenous ACh by a brief (30 min) incubation with 20 μM HC-3, which did not cause death of more than 10% cells, as determined by the trypan blue dye exclusion assay. After that, the cells were fed with KGM containing 10 ng/ml EGF as well as an α9 agonist in the presence or absence of antagonists. In some experiments, we used human KCs transfected with siRNA-α9 *vs.* siRNA-NC or α9−/− *vs.* α9 +/+ murine KCs. After incubation for various time points (see Results), the cells were lysed and used in biochemical assays. The activities of Src, EGFR kinase, PLC, PKC, Rho and Rac were measured in accordance to the protocols provided by the manufacturers. The levels of phosphorylation of FAK, paxillin, β-catenin, desmoglein 3 and cytokeratins were assayed by quantitative western blot using anti-phosphoprotein antibodies to FAK, paxillin and β-catenin or *via* immunoprecipitation coupled western blotting (see below).

Cell scattering assay was performed in the 6-well cell and tissue culture plates in accordance to the procedures detailed elsewhere [17,18]. Briefly, at least 10 colonies comprised by at least 8 KCs tightly attached to one another were examined before and after each experimental treatment. Cell scattering (colony dispersion) was documented by photography. The degree of colony dispersion was expressed as "+" (singe cell break away, <10% dissociated cells), "++" (partial colony dissociation, 10–75% dissociated cells) and "+++" (complete dissociation, >75% dissociated cells).

Scratch assay was performed using our modification [19] of the original assay [20]. Briefly, confluent monolayers in 6-well dishes were scratched with a 100 μl pipette tip and incubated at 37°C and 5% CO_2 in air until complete re-epithelialization of wounded monolayer in one of the cultures, but no longer than 24 h. To inhibit proliferation, for the first 2 h of incubation KCs were fed with KGM containing 10 μg/ml mitomycin-C (Sigma-Aldrich, Inc.). The extent of epithelialization was documented by photography, and the amount of migration was quantitated by computer-assisted image analysis software IP Lab (Scanalytics, Fairfax, VA).

Colony outgrowth assay measured the random migration distance in agarose gel keratinocyte outgrowth system (**AGKOS**), as detailed by us elsewhere [21,22]. Briefly, a confluent keratinocyte monolayer was formed by loading KCs at a high density (4×10^4 cells/10 μl) into 3 mm well in an agarose gel and incubating the cultures at 1.2 mM Ca^{2+} in KGM to allow the cells to adhere to the dish bottom and form intercellular junctions. After starvation of EGF and deprivation of endogenous ACh by HC-3, as described above, the migration was initiated by feeding the cells with KGM containing EGF and test cholinergic drugs. The cultures were incubated for 10 d in a humid CO_2 incubator with daily changes of medium. Some KCs were first transfected with siRNA. To standardize results obtained in experiments using KCs from different donors, the mean values of the migration distances were converted into the percentage of control. The control value for KCs from each particular donor was determined by measuring the baseline migration distance (in mm) and taken as 100%.

Keratinocyte adhesion assays

Cell-matrix attachment was quantified using our original computerized microassay [14]. Briefly, KCs suspended in KGM containing test compounds were loaded in 96-well cell and tissue culture plates at a concentration of 2.5×10^4/well, incubated for 1 h in a humid 5% CO_2 incubator at 37°C, washed, fixed, stained with crystal violet, and decolorized with sodium dodecyl sulfate. The optical density (**OD**) of the crystal violet dye retained by the cells attached to the wells was measured *in situ* at 590 nm on ELISA-plate reader. The more KCs attached to well, the higher the OD values were obtained.

Cell-cell attachment was measured using the monolayer permeability assay [23,24]. Briefly, a confluent keratinocyte monolayer was formed in Transwell-COL (Costar, Cambridge, MA) chambers inserted into the 24-well tissue culture plates. KCs were seeded at a cell density of 1×10^4/100 μl KGM and cultivated at 37°C in humid atmosphere with 5% CO_2 for 7–12 days. Confluent monolayers were fed with KGM containing test compounds. Some monolayers were first dissociated due to a brief (30 sec) exposure to 0.53 mM EDTA, and some cells were first transfected with siRNA and then used in experiments. After 1 h of incubation with test compounds, the permeability of the monolayer was measured by adding 100 μl KGM containing [^{3}H]thymidine (**[^{3}H]dT**; 1 μCi/insert; 6.7 Ci/mmol; NEN) to each culture. Five minutes later, 100 μl aliquots of solution containing [^{3}H]dT were taken in triplicate from each lower chamber. The more cells detached from each other and rounded up, the more tracer penetrated to the lower chamber through the porous membrane of the upper chamber, and the higher the permeability coefficient (**PC**) values were obtained. The PC was defined as:

$$\mathrm{PC} = \frac{\text{cpm in experimental culture}}{\text{cpm in control culture}} \times 100.$$

In vivo wounding and morphometric assay of epithelialization rate

The assay of the skin wound epithelization rate was performed in accordance to the established protocol [19]. Briefly, using a uniform 1 × 1 cm square template, full thickness excisions through the panniculus carnosus were made on the anesthetized skin of 6–7 weeks old α9−/− and α9+/+ littermates, in whom the hair cycle had been synchronized by the anagen induction technique [25]. Each animal received 2 wounds at the symmetric sites of the central back, 0.5 cm off the vertebral line. Wounds were left undressed, and wounded animals were individually housed under aseptic conditions for 2, 4, 6, 8 and 10 d, after which the mice were euthanized, and the wound border was harvested by shaving a narrow strip along the perimeter of the wound. At least 3 animals per time point and genotype were used. The rate of epithelialization was assayed in hematoxylin and eosin stained cryostat sections from the middle of the wound by measuring the lengths of the tongues of new epithelium extending from either side of the wound.

siRNA transfection experiments

For transfection with siRNAs, we followed the standard protocol described in detail elsewhere [26]. Briefly, KCs were treated with increasing concentrations of siRNA in the transfection solution with the DharmaFECT™ 1 siRNA Transfection Reagent (Dharmacon) for 16 h at 37° C in a humid, 5% CO_2 incubator. On the next day, the transfection medium was replaced by KGM, and the cells were incubated for 72 h to determine at which time point maximum inhibition of the receptor protein expression occurs. The siRNA transfection efficiency was also assayed using FITC-labeled luciferase GL2 duplex (Dharmacon). It was experimentally established that maximal, i.e., >90%, inhibition of α9 expression occurred 48 hrs after transfection (data not shown), at which point the cells were used in all experiments.

Immunoprecipitation and Western blot assays

KCs were scraped from the bottom of the dishes and placed in lysis buffer (0.1 M NaCl, 10 mM Tris, pH 7.6, 1 mM EDTA, 0.2% NP-40, 1 μg/ml aprotinin, 2 mM Na_3VO_4, and 1 mM PMSF). Samples were homogenized, and protein concentration determined using a Bio-Rad protein assay kit. Anti-desmoglein 3 or anti-pan cytokeratin antibody was added to cell lysate, and the preparation was gently rocked at 4°C overnight. A protein G agarose bead slurry (Protein G Immunoprecipitation Kit; Sigma-Aldrich Corp. Inc.) was added and incubated at 4°C for 2 h. Beads were collected by pulsing 5 s in a microcentrifuge at 14,000 rpm, and rinsed three times with ice-cold cell lysis buffer. The agarose beads were resuspended in SDS-sample buffer (0.5 M Tris–HCl, 10% SDS, 10% glycerol, 2.5% bromophenol blue, 5% β-mercaptoethanol). Protein samples were boiled and separated on 7.5% SDS-polyacrylamide gels. Proteins were transferred to nitrocellulose, blocked overnight with 1.5% bovine serum albumin in Tris-buffered saline (**TBS**; 10 mM Tris–HCl, 150 mM NaCl, pH 8.0), and incubated for 1 h with the phosphoserine antibody. Control blots stained with either anti-desmoglein 3 or anti-pan cytokeratin antibody were run as loading controls. After washing in TBS with 0.1% Tween-20, the membranes were incubated with a secondary antibody, and then developed using the ECL + Plus chemiluminescent detection system (Amersham Pharmacia Biotech, Inc., Piscataway, NJ). To visualize antibody binding, the membranes were scanned with Storm™/ FluorImager (Molecular Dynamics, Mountain View, CA), and band intensities were determined by area integration using ImageQuant software [27].

Statistical analysis

All experiments were performed in triplicates and the results were expressed as mean ± SD. Statistical significance was determined using Student's *t*-test. Differences were deemed significant if the calculated p value was <0.05.

RESULTS

Inactivation of keratinocyte α9 AChR delays wound healing in vitro and in vivo

To evaluate the role of α9 AChR in mediating cholinergic effects on keratinocyte migration and wound epithelialization, we employed the established models of wound healing *in vitro* and *in vivo*. The keratinocyte monolayers were used in the scratch assay and the α9−/− vs. α9 +/+ mice in skin wounding experiments. Exposure of keratinocyte monolayers to exogenous ACh (1 mM) or the α9 agonist MCC (0.1 mM) did not alter the rate of epithelialization ($p>0.05$) (Fig. 1A), suggesting that keratinocyte AChRs are saturated by the endogenously produced and secreted ACh. When ACh synthesis was inhibited with HC-3 (20 μM) or when α9 AChR was blocked with the antagonists Str (0.1 μM) and ICS (0.1 μM) given alone or as a mixture, the epithelialization rate was significantly ($p<0.05$) delayed, compared to intact control cultures (Fig. 1A). The inhibitory effect HC-3 could be abolished when the monolayers were treated with ACh or MCC given alone but not in combination with antagonists. The hypothesis that the observed effects were due to α9 ligation was confirmed in experiments with KCs transfected with siRNA-α9, but not siRNA-NC. Silencing of the α9 gene led to significant ($p<0.05$) reduction of epithelialization rate (Fig. 1A). Likewise, functional inactivation of α9 by null mutation slowed the rate of epithelialization of incisional wounds in α9 knockout mice, compared to that found in wild-type littermates (Fig. 1B–D). However, a significant ($p<0.05$) lag in wound epithelialization was observed only during the first days after wounding, suggesting that α9 AChR was involved in regulation of early events of keratinocyte migration.

Critical role of α9 AChR in migration initiation

Microscopic observation of the wound edge in the scratch assay and the megacolony leading edge in the AGKOS plates in both cases revealed that inhibition of α9 AChR altered the ability

of KCs to initiate migration. Although KCs elongated, extended lamellipodium, produced filopodia and moved out from the culture substrate, most of them remained anchored to the substrate by long cytoplasmic processes that stretched during migration instead of the cells retracting their uropod (Fig. 2). These visual observations were corroborated by results of quantitative assays of migration initiation. Both pharmacologic blockade of α9 AChR and its functional inactivation by RNA interference diminished the extent of colony dispersion induced by HGF/SF (Table 1). The role of α9 AChR in migration initiation was also measured in AGKOS assay after stimulating cells with EGF. The outgrowth of KCs from the megacolony was significantly inhibited ($p<0.05$) when the cells were deprived of endogenous ACh or when α9 AChR signaling was blocked (Fig. 1E). Taken together, these results suggested that α9 AChR plays a critical role in cholinergic autocrine and paracrine regulation of the keratinocyte functions mediating the earliest events in lateral migration, such as modifications of cell-matrix and cell-cell attachments.

α9 AChR controls cell adhesion

To evaluate the role of α9 AChR signaling in assembly/disassembly of the cell-matrix and cell-cell adhesion complexes, we employed quantitative assays of keratinocyte adhesion to plastic and monolayer permeability, respectively. Stimulation of suspended KCs with exogenously added ACh or MCC accelerated cell attachment to the dish bottom (Fig. 3A). Pharmacologic blockade of α9 AChR with Str and ICS, gene silencing with siRNA-α9 and null mutation of the α9 gene significantly ($p<0.05$) inhibited the adhesive function of KCs. The ability of suspended KCs to attach to the substrate was diminished (Fig. 3A), revealing a problem with assembly and function of focal adhesions. The permeability of the monolayers was increased (Fig. 3B), revealing the problems with maintaining the polygonal cell shape and cell-cell cohesion. In the past, blocking of α9 AChR in confluent monolayers has been shown to cause shrinkage of KCs [13]. This decreases the area occupied by a cell and causes gaps between the cells, which increased monolayer permeability [23]. When the confluent monolayer was first dissociated due to a brief exposure to EDTA and then stimulated with ACh, the impermeability of the monolayer rapidly restored (Fig. 3C). Surprisingly, the effect of MCC on dissociated KCs was quite different. The permeability of MCC exposed cultures increased even higher. Instead of flattening, spreading the cytoplasm and establishing intercellular contacts, as did ACh-treated cells, the KCs exposed to MCC acquired the letter “D”-like morphology normally observed for the migratory pattern, due to unilateral extension of the lamellipodium (not shown). In the presence of the α9 antagonists Str and ICS, the permeability of the monolayers was even higher (Fig. 3C). The majority of cells in these cultures remained small, rounded up and completely separated from one another (not shown).

Effects of α9 AChR activation on phosphorylation of adhesion and cytoskeletal proteins

Because phosphorylation of adhesion and cytoskeletal molecules plays a critical role in normal function of cell adhesion complexes, we performed a time-course analysis of the phosphorylation state of adhesion molecules comprising focal adhesions (FAK, paxillin) and intercellular junctions (β-catenins, desmoglein 3), and cytokeratins forming the intermediate filament framework. Stimulation of α9 AChR upregulated the degree of phosphorylation of these proteins in a time-dependent fashion. The phosphorylation level of FAK reached its peak at 30 min, that of paxillin and β-catenin at 60 min, desmoglein 3 at 120 and cytokeratin at 180 min after exposure of KCs to MCC (Fig. 4A, B). The specificity of observed changes in phosphorylation to activation of α9 AChR was demonstrated by abolishing the effects of MCC with the α9 antagonists Str and ICS, and due to transfection with siRNA-α9, but not siRNA-NC (Fig. 4C). These results indicated that signaling downstream of α9 AChR involves activation of signaling kinases.

Time-course study of kinase activities following α9 AChR activation

Signaling downstream of α9 AChR was investigated in a time-course study of the activities of serine/threonine and tyrosine kinases, PLC and small GTPases. Stimulation of α9 AChR with MCC led to activation of several kinases, including Src that peaked at 15 min, EGFR—at 30 min, PLC—at 60 min and PKC—at 90 min, as well as activation of Rho and Rac (Fig. 5), all of which could be abolished in the presence of receptor antagonists and due to inhibition of the α9 gene expression (Fig. 4D). These results identified signaling kinases and small GTPases involved in the α9 AChR coupled pathways that regulate shape and adhesion of KCs during initiation of their lateral migration.

DISCUSSION

The results of this study demonstrated for the first time that signaling downstream of α9 AChR is critical for initiation of lateral migration of KCs. The α9 receptor directly regulates cell-matrix and cell-cell adhesion through the signaling pathways that involve Src, EGFR kinase, PLC, PKC, Rho and Rac. The end result includes changes on the phosphorylation status of the adhesion molecules comprising focal adhesions and intercellular junctions, as well as cytokeratins. In the past, we identified the human homolog of rat α9 AChR and raised rabbit monoepitopic antibody that visualized α9 at the sites of cell-cell attachments where this receptor can be targeted by anti-keratinocyte antibodies produced by patients with pemphigus vulgaris [13]. Pemphigus is an autoimmune blistering disease altering intercellular adhesion in the stratified squamous epithelium in which patients develop extensive blisters reminiscent of severe burns. In the epidermis, α9 is one of the most abundant AChR subtypes, being expressed predominantly by suprabasal (prickle) KCs [13,28] that are believed to be the most mobile cells, since they have to constantly assemble and disassemble their adherens and desmosomal junctions to allow for upward migration through the epidermal layers [29].

The α9 subunit is capable of forming functional homomeric AChR channels as well as a heteromeric channel with α10 [4,6]. Although α9 shares about 40% sequence homology with all other known nicotinic AChR subunits [4], it forms homo- and heteropentameric channels that undergo conformational changes upon binding of both nicotinic and muscarinic drugs, as well as ligands of the type A γ-aminobutyric acid, glycine, and type 3 serotonin receptors [4, 9,30]. The observed effects could be due to activation of α9α10 AChR, since it is the most likely functional receptor in vivo [6,30–32]. As a consequence of the ablation of α9 expression by siRNA or gene knockout strategies only α10 would be left, which is non-functional. Therefore, the expected results from ablation of α9 if the keratinocyte receptor were an α9 homomer would be the same to the scenario where the receptor is an α9α10 heteromer.

While most cholinergic agonists act at α9 AChRs as pharmacologic antagonists, MCC mimics the agonistic action of ACh [8]. MCC can also activate the ACh gated ion channels comprised by α4 and β2 subunits [33,34], but this nicotinic AChR subtype is not expressed by KCs (reviewed in [3]). The α9 AChR can be selectively blocked with the glycine receptor inhibitor Str and the $5HT_3$ serotonin receptor antagonist ICS [9,10]. Str and ICS block both α9 and α9α10 receptors in heterologous systems. While the potencies of these drugs for α9 AChR and their typical target receptors are similar, the affinity of strychnine binding to α9 is slightly higher then that of ICS [9]. In this study, we used these two antagonists either alone or as a mixture and found no additive effects. Therefore, receptors other than α9 AChR were not involved in the effects of MCC and test antagonists on keratinocyte adhesion and motility observed in this study.

Activation of α9 AChR accelerated attachment of suspended KCs to the culture substrate, which is an important element of the cell migratory function. However, in a previous study, we found that inactivation of α9 signaling does not alter the rate of crawling locomotion of

KCs [22]. This seeming controversy is explained by the fact that signaling through α9 AChR is critical during the earliest phase of crawling locomotion when KCs free themselves from the culture substrate and move out. To complete this essential step of wound epithelialization, KCs should disable their connections with neighboring cells and extracellular matrix. Inhibition of α9 AChR altered the ability KCs to break away from the culture substrate in the scratch assay and move out from the megacolony in the AGKOS assay. These alterations of the keratinocyte migratory function may explain the delayed epithelialization of skin wounds inflicted in α9−/− mice, compared to their α9+/+ littermates. No obvious defects in cell-ECM or cell-cell adhesion have been observed in α9 −/− mice. In contrast to in vitro experiments, wherein acute inhibition of α9 was achieved by pharmacologic antagonists or siRNA-α9 transfection, the in vivo experiments were performed in knockout mice that lacked α9 function chronically. By analogy with α7 knockout mice that show upregulated expression of non-α7 AChR subunits [16], chronic abrogation of α9 signaling might result in partial compensation of the missing receptor function through alternative nicotinergic pathways.

Stimulation of α9 AChR produced different effects on KCs in a confluent monolayer, compared to KCs in dissociated culture. While MCC did not affect impermeability of confluent monolayer, it prevented re-attachment of KCs in the cultures dispersed by EDTA. The MCC treated cells acquired a migratory shape, instead of the polygonal shape observed in ACh treated cultures. In the presence of α9 antagonists, MCC treated KCs did not spread their cytoplasmic aprons and remained rounded up, which is in keeping with earlier observations that blockade of α9 with pharmacologic antagonists or rabbit anti-α9 antibody causes keratinocyte shrinkage and dyshesion [13,24,35]. Therefore, it can be concluded that in a confluent monolayer of KCs, α9 signaling maintains polygonal cell shape and intercellular adhesion of KCs, whereas activation of α9 AChR in dispersed cells facilitates their lateral migration.

The differences in effects of ACh, which activates all AChR subtypes, and the α9 preferring agonist MCC on keratinocyte cell-cell cohesion can be explained by the fact that cholinergic control of the adhesive function of KCs is mediated by the synergistic action of α9 and α3 nicotinic AChRs together with the M_3 muscarinic AChR subtype. There are apparent differences in the end results of signaling downstream of each of these receptors. For instance, while simultaneous silencing of α9, α3 and M_3 decreased the relative amounts of E-cadherin by more than 35%, and that of β- and γ-catenins by 34 and 20%, respectively, the KCs comprising the stratified epithelium of α9 knockout mice exhibited an approximately 2.5-fold elevation of E-cadherin [24]. This upregulated expression of classical cadherins might contribute to failure of KCs with blocked α9 AChR to break away from the culture substrate, and consequently to delayed wound epithelization *in vitro* and *in vivo*. It is also noteworthy that in contrast to α3−/− and M_3−/− mice, the α9−/− mice do not show any gross or microscopic signs of altered keratinocyte adhesion [24]. Furthermore, it has been recently demonstrated that in addition to the adhesion molecules comprising adherens and desmosomal junctions, such as desmogleins 1 and 3, desmocollin and desmoplakin, α9 AChR signaling is also important for normal expression of the tight junction proteins ZO-1 and claudin 4 [35].

Diverse biologic effects of the AChR subtypes involved in the physiologic control of keratinocyte adhesion and motility are apparently mediated by distinct signaling pathways uniquely coupled by each AChR subtype under consideration. The Ca^{2+} permeability of ion channels comprised of α9 subunits is relatively high, suggesting that one of the main functions of this channel is to provide a pathway for Ca^{2+} influx [36,37]. Results of this study demonstrated that stimulation of α9 AChR activates signaling kinases in a specific temporal fashion, with Src and EGFR kinases peaking at early (15 and 30 min) and PKC at late (90 min) time points. Since the peak of Rho and Rac activities occurred at 60 min post-stimulus, these GTPases were likely activated secondary to upstream events mediated by Src and/or EGFR signaling. Src family kinases can couple receptors lacking intrinsic kinase activity to receptor

tyrosine kinases (**RTKs**). For example, activation of Src relays the signal emanating from the interaction of ouabain with Na^+/K^+-ATPase to the EGFR [38]. Involvement of PKC in the signaling pathway downstream from α9 AChR might be a result of Ca^{2+}-dependent events, such as activation of PLC that preceded that of PKC, and/or due to an increase of diacylglycerol (reviewed in [39]).

Activation of α9 AChR signaling elevated the phosphorylation status of the adhesion molecules, which is in keeping with a report that activation of α9 AChR induces phosphorylation of cell membrane-associated proteins [40]. The focal adhesion molecules FAK and paxillin were phosphorylated on the tyrosine residue whereas the adherens junction protein β-catenin, and the desmosomal protein desmoglein 3 were phosphorylated on the serine residue. Maximal phosphorylation of FAK and paxillin occurred within 60 min after α9 stimulation, suggesting the direct involvement of Src and RTKs known to act either independently or in concert to regulate cell adhesion [41]. It has been demonstrated that Src can activate FAK by its phosphorylation on Tyr^{577}, measured in this study, and form complexes with activated FAK [42]. RTKs can elicit the dismantling of intercellular junctions and cause a dramatic change in cell morphology and gene expression in which cells shift from an epitheliod to a migratory phenotype and initiate migration, as in cancer metastasis [43].

Phosphorylation of focal adhesion proteins is required for normal reorganization of integrin-cytoskeletal interactions in a crawling cell [44]. Phosphorylation of paxillin and FAK controls cell polarization and motility [45–47]. Paxillin phosphorylation is an early and requisite step in cell spreading preceding migration [48]. EGFR stimulation leads to phosphorylation of paxillin followed by activation of Rac, which promotes cell motility [49]. In fact, the β-catenin phosphorylation that peaked at the 60^{th} min apparently required involvement of intermediate components, such as the serine/threonine kinase Rac. Indeed, β-catenin is a known target of EGFR-dependent phosphorylation [50]. FAK phosphorylation maybe critical for the turnover of the focal complexes that facilitates disassembly of the focal contact in the trailing edge (uropod), thus allowing a cell to move forward (reviewed in [51]). The retracting fibers are characteristic structures of the uropod formed in cell migration during rear release [52]. Since we observed a failure of uropod retraction, it is of importance to know whether the retracting fibers are actually formed in cells with inactive α9 AChR. Unfortunately, this issue could not be resolved in this study due to technical limitations.

The “late targets” of α9-dependent phosphorylation are desmoglein 3 and cytokeratin, which could be substrates for PKC and Rho-kinase (**ROK**). PKC-dependent phosphorylation of desmosomal protein plays an important role in assembly and disassembly of desmosomal junctions [53–55]. Likewise, cytokeratin hyperphosphorylation is a key to the modification of cell shape accommodating functional requirements [56,57]. Since α9 is one of a number of self-antigens targeted by autoantibodies produced in patients with pemphigus [13], it is of interest that binding of pemphigus antibodies to KCs induces signaling that involves PKC and causes phosphorylation and inactivation of desmoglein 3 [58–61]. Rho is also involved in the regulation of desmosomal adhesion by maintaining the cytoskeletal anchorage of desmosomal proteins, and pemphigus antibodies cause cell detachment, in part, by interfering with Rho-mediated signaling [62]. It is well known, however, that Rho and Rac exert mutually antagonistic effects in the cell motility processes (reviewed in [63]). RhoA is essential for the formation of focal adhesions and its function can be antagonized by Rac1 [64,65]. Rac is essential for the protrusion of lamellipodia and for forward movement [66]. We have previously demonstrated engagement of Rac/Cdc42 and Rho/ROK pathways in the signaling cascade mediating cholinergic effects on keratinocyte motility through non-α9 AChRs [19,22], which, taken altogether, suggests that signaling pathways downstream of the AChR subtypes involved in regulation of related cellular functions of KCs, such as adhesion and migration, elicit biologic effects through divergent modifications of the same and/or associated effector molecules and

structural proteins. At this point, it is difficult to decide which of the pathways checked by us is coupled uniquely to regulation of cell-cell vs. cell-matrix adhesion, or both. Future mechanistic studies employing pharmacologic and molecular inhibitors should answer this intriguing question.

In summary, our data indicate that α9 AChR plays a key role in regulating early events of keratinocyte migration by modulating the phosphorylation levels of the adhesion and cytoskeletal proteins. These findings, together with our earlier observations of α9 effects on the gene expression of adhesion molecules [24], suggest that signaling through α9 AChR helps maintain a dynamic equilibrium between assembly and disassembly of adhesion complexes, both of the cell-matrix and cell-cell types, through transcriptional, translational and postranslational modifications of the structural and effector molecules that determine cell shape, cytoplasm motility and adhesive properties of KCs. The involvement of diverse effector mechanisms downstream of α9 AChR may facilitate cycling between the phosphorylated and dephosphorylated states required to achieve a fine balance between detachment of the uropod from culture substrate and attachment of lamellipodium in a crawling cell, as well as between detachment from neighboring cells at the beginning of migration and re-attachment once the epithelialization has been completed. Therefore, it appeared that the effects of α9 AChR are different at different stages of epithelialization. α9 AChR signaling may be equally important in regulating other biological process related to the cell adhesive function, such as tissue morphogenesis and maintenance of tissue architecture and polarity, as well as limiting cell movement and proliferation. Hence, pharmacologically manipulating α9 AChR signaling could aid in the development of novel methods useful for treatments of wounds that fail to heal, diseases of skin adhesion, and tumor metastasis.

Acknowledgements

This work was supported by the NIH grant GM62136 (to S.A.G.).

References

1. Woodley, DT. Reepithelialization. In: Clark, RAF., editor. The Molecular and Cellular Biology of Wound Repair. Plenum Press; New York: 1996.
2. Jensen PJ, Wheelock MJ. The relationships among adhesion, stratification and differentiation in keratinocytes. Cell Death Differ 1996;3:357–371. [PubMed: 17180106]
3. Grando SA, Pittelkow MR, Schallreuter KU. Adrenergic and cholinergic control in the biology of epidermis: physiological and clinical significance. J Invest Dermatol 2006;126:1948–1965. [PubMed: 16912692]
4. Elgoyhen AB, Johnson DS, Boulter J, Vetter DE, Heinemann S. α9: An acetylcholine receptor with novel pharmacological properties expressed in rat cochlear hair cells. Cell 1994;79:705–715. [PubMed: 7954834]
5. Wikstrom MA, Lawoko G, Heilbronn E. Cholinergic modulation of extracellular ATP-induced cytoplasmic calcium concentrations in cochlear outer hair cells. J Physiol Paris 1998;92:345–349. [PubMed: 9789835]
6. Elgoyhen AB, Vetter DE, Katz E, Rothlin CV, Heinemann SF, Boulter J. α10: A determinant of nicotinic cholinergic receptor function in mammalian vestibular and cochlear mechanosensory hair cells. Proc Natl Acad Sci U S A 2001;98:3501–3506. [PubMed: 11248107]
7. Grando SA. Cholinergic control of epidermal cohesion in norm and pathology. Exp Dermatol 2006;15:265–282. [PubMed: 16512874]
8. Verbitsky M, Rothlin CV, Katz E, Belen Elgoyhen A. Mixed nicotinic-muscarinic properties of the α9 nicotinic cholinergic receptor. Neuropharmacology 2000;39:2515–2524. [PubMed: 11044723]
9. Rothlin CV, Katz E, Verbitsky M, Elgoyhen AB. The α9 nicotinic acetylcholine receptor shares pharmacological properties with type A gamma-aminobutyric acid, glycine, and type 3 serotonin receptors. Mol Pharmacol 1999;55:248–254. [PubMed: 9927615]

10. Rothlin CV, Lioudyno MI, Silbering AF, Plazas PV, Casati ME, Katz E, Guth PS, Elgoyhen AB. Direct interaction of serotonin type 3 receptor ligands with recombinant and native alpha 9 alpha 10-containing nicotinic cholinergic receptors. Mol Pharmacol 2003;63:1067–1074. [PubMed: 12695535]
11. Guyenet P, Lefresne P, Rossier J, Beaujouan JC, Glowinski J. Inhibition by hemicholinium-3 of (14C) acetylcholine synthesis and (3H)choline high-affinity uptake in rat striatal synaptosomes. Mol Pharmacol 1973;9:630–639. [PubMed: 4788157]
12. Veldsema-Currie RD, Labruyere WT, Langemeijer MW. Depletion of total acetylcholine by hemicholinium-3 in isolated rat diaphragm is less in the presence of dexamethasone. Brain Res 1984;324:305–312. [PubMed: 6529621]
13. Nguyen VT, Ndoye A, Grando SA. Novel human α9 acetylcholine receptor regulating keratinocyte adhesion is targeted by pemphigus vulgaris autoimmunity. Am J Pathol 2000;157:1377–1391. [PubMed: 11021840]
14. Grando SA, Cabrera R, Hostager BS, Bigliardi PL, Blake JS, Herron MJ, Dahl MV, Nelson RD. Computerized microassay of keratinocyte cell-plastic attachment and proliferation for assessing net stimulatory inhibitory and toxic effects of compounds on nonimmortalized cell lines. Skin Pharmacol 1993;6:135–147. [PubMed: 8352951]
15. Vetter DE, Liberman MC, Mann J, Barhanin J, Boulter J, Brown MC, Saffiote-Kolman J, Heinemann SF, Elgoyhen AB. Role of α9 nicotinic ACh receptor subunits in the development and function of cochlear efferent innervation. Neuron 1999;23:93–103. [PubMed: 10402196]
16. Arredondo J, Nguyen VT, Chernyavsky AI, Bercovich D, Orr-Urtreger A, Kummer W, Lips K, Vetter DE, Grando SA. Central role of α7 nicotinic receptor in differentiation of the stratified squamous epithelium. J Cell Biol 2002;159:325–336. [PubMed: 12391028]
17. Russell AJ, Fincher EF, Millman L, Smith R, Vela V, Waterman EA, Dey CN, Guide S, Weaver VM, Marinkovich MP. Alpha 6 beta 4 integrin regulates keratinocyte chemotaxis through differential GTPase activation and antagonism of alpha 3 beta 1 integrin. J Cell Sci 2003;116:3543–3556. [PubMed: 12865436]
18. McCawley LJ, O'Brien P, Hudson LG. Epidermal growth factor (EGF)- and scatter factor/hepatocyte growth factor (SF/HGF)- mediated keratinocyte migration is coincident with induction of matrix metalloproteinase (MMP)-9. J Cell Physiol 1998;176:255–265. [PubMed: 9648913]
19. Chernyavsky AI, Arredondo J, Wess J, Karlsson E, Grando SA. Novel signaling pathways mediating reciprocal control of keratinocyte migration and wound epithelialization by M_3 and M_4 muscarinic receptors. J Cell Biol 2004;166:261–272. [PubMed: 15263021]
20. Cha D, O'Brien P, O'Toole EA, Woodley DT, Hudson LG. Enhanced modulation of keratinocyte motility by transforming growth factor-alpha (TGF-alpha) relative to epidermal growth factor (EGF). J Invest Dermatol 1996;106:590–597. [PubMed: 8617990]
21. Grando SA, Crosby AM, Zelickson BD, Dahl MV. Agarose gel keratinocyte outgrowth system as a model of skin re-epithelization: requirement of endogenous acetylcholine for outgrowth initiation. J Invest Dermatol 1993;101:804–810. [PubMed: 8245509]
22. Chernyavsky AI, Arredondo J, Marubio LM, Grando SA. Differential regulation of keratinocyte chemokinesis and chemotaxis through distinct nicotinic receptor subtypes. J Cell Sci 2004;117:5665–5679. [PubMed: 15494367]
23. Grando SA, Dahl MV. Activation of keratinocyte muscarinic acetylcholine receptors reverses pemphigus acantholysis. J Eur Acad Dermatol Venereol 1993;2:72–86.
24. Nguyen VT, Chernyavsky AI, Arredondo J, Bercovich D, Orr-Urtreger A, Vetter DE, Wess J, Beaudet AL, Kitajima Y, Grando SA. Synergistic control of keratinocyte adhesion through muscarinic and nicotinic acetylcholine receptor subtypes. Exp Cell Res 2004;294:534–549. [PubMed: 15023540]
25. Paus R, Stenn KS, Link RE. Telogen skin contains an inhibitor of hair growth. Br J Dermatol 1990;122:777–784. [PubMed: 2369558]
26. Chernyavsky AI, Arredondo J, Karlsson E, Wessler I, Grando SA. The Ras/Raf-1/MEK1/ERK signaling pathway coupled to integrin expression mediates cholinergic regulation of keratinocyte directional migration. J Biol Chem 2005;280:39220–39228. [PubMed: 16150734]

27. Arredondo J, Chernyavsky AI, Jolkovsky DL, Pinkerton KE, Grando SA. Receptor-mediated tobacco toxicity: cooperation of the Ras/Raf-1/MEK1/ERK and JAK-2/STAT-3 pathways downstream of α7 nicotinic receptor in oral keratinocytes. FASEB J 2006;20:2093–2101. [PubMed: 17012261]
28. Kurzen H, Berger H, Jager C, Hartschuh W, Naher H, Gratchev A, Goerdt S, Deichmann M. Phenotypical and molecular profiling of the extraneuronal cholinergic system of the skin. J Invest Dermatol 2004;123:937–949. [PubMed: 15482483]
29. Wolff K, Wolff-Schreiner EC. Trends in electron microscopy of skin. J Invest Dermatol 1976;67:39–57. [PubMed: 778296]
30. Plazas PV, Katz E, Gomez-Casati ME, Bouzat C, Elgoyhen AB. Stoichiometry of the alpha9alpha10 nicotinic cholinergic receptor. J Neurosci 2005;25:10905–10912. [PubMed: 16306403]
31. Lustig LR, Peng H, Hiel H, Yamamoto T, Fuchs PA. Molecular cloning and mapping of the human nicotinic acetylcholine receptor alpha10 (CHRNA10). Genomics 2001;73:272–283. [PubMed: 11350119]
32. Sgard F, Charpantier E, Bertrand S, Walker N, Caput D, Graham D, Bertrand D, Besnard F. A novel human nicotinic receptor subunit, α10, that confers functionality to the α9-subunit. Mol Pharmacol 2002;61:150–159. [PubMed: 11752216]
33. Aubert I, Cecyre D, Gauthier S, Quirion R. Comparative ontogenic profile of cholinergic markers, including nicotinic and muscarinic receptors, in the rat brain. J Comp Neurol 1996;369:31–55. [PubMed: 8723701]
34. Wang DX, Abood LG. Expression and characterization of the rat alpha 4 beta 2 neuronal nicotinic cholinergic receptor in baculovirus-infected insect cells. J Neurosci Res 1996;44:350–354. [PubMed: 8739154]
35. Kurzen H, Henrich C, Booken D, Poenitz N, Gratchev A, Klemke CD, Engstner M, Goerdt S, Maas-Szabowski N. Functional characterization of the epidermal cholinergic system in vitro. J Invest Dermatol 2006;126:2458–2472. [PubMed: 16810300]
36. Katz E, Verbitsky M, Rothlin CV, Vetter DE, Heinemann SF, Elgoyhen AB. High calcium permeability and calcium block of the alpha9 nicotinic acetylcholine receptor. Hear Res 2000;141:117–128. [PubMed: 10713500]
37. Fucile S, Sucapane A, Eusebi F. Ca2+ permeability through rat cloned alpha9-containing nicotinic acetylcholine receptors. Cell Calcium 2006;39:349–355. [PubMed: 16451809]
38. Haas M, Wang H, Tian J, Xie Z. Src-mediated inter-receptor cross-talk between the Na+/K+-ATPase and the epidermal growth factor receptor relays the signal from ouabain to mitogen-activated protein kinases. J Biol Chem 2002;277:18694–18702. [PubMed: 11907028]
39. Albert PR. Dopamine-D2-mediated inhibition of TRH-induced PLC activation in pituitary cells-direct or indirect? Endocrinology 2002;143:744–746. [PubMed: 11861491]
40. Szonyi M, Csermely P, Sziklai I. Acetylcholine-induced phosphorylation in isolated outer hair cells. Acta Otolaryngol 1999;119:185–188. [PubMed: 10320073]
41. Mariner DJ, Davis MA, Reynolds AB. EGFR signaling to p120-catenin through phosphorylation at Y228. J Cell Sci 2004;117:1339–1350. [PubMed: 14996911]
42. Lin EH, Hui AY, Meens JA, Tremblay EA, Schaefer E, Elliott BE. Disruption of Ca2+-dependent cell-matrix adhesion enhances c-Src kinase activity, but causes dissociation of the c-Src/FAK complex and dephosphorylation of tyrosine-577 of FAK in carcinoma cells. Exp Cell Res 2004;293:1–13. [PubMed: 14729052]
43. Boyer B, Tucker GC, Valles AM, Franke WW, Thiery JP. Rearrangements of desmosomal and cytoskeletal proteins during the transition from epithelial to fibroblastoid organization in cultured rat bladder carcinoma cells. J Cell Biol 1989;109:1495–1509. [PubMed: 2677020]
44. Schoenwaelder SM, Burridge K. Bidirectional signaling between the cytoskeleton and integrins. Curr Opin Cell Biol 1999;11:274–286. [PubMed: 10209151]
45. Romanova LY, Hashimoto S, Chay KO, Blagosklonny MV, Sabe H, Mushinski JF. Phosphorylation of paxillin tyrosines 31 and 118 controls polarization and motility of lymphoid cells and is PMA-sensitive. J Cell Sci 2004;117:3759–3768. [PubMed: 15252114]
46. Vindis C, Teli T, Cerretti DP, Turner CE, Huynh-Do U. EphB1-mediated cell migration requires the phosphorylation of paxillin at Tyr-31/Tyr-118. J Biol Chem 2004;279:27965–27970. [PubMed: 15107421]

47. Bianchi M, De Lucchini S, Marin O, Turner DL, Hanks SK, Villa-Moruzzi E. Regulation of FAK Ser-722 phosphorylation and kinase activity by GSK3 and PP1 during cell spreading and migration. Biochem J 2005;391:359–370. [PubMed: 15975092]
48. Richardson A, Malik RK, Hildebrand JD, Parsons JT. Inhibition of cell spreading by expression of the C-terminal domain of focal adhesion kinase (FAK) is rescued by coexpression of Src or catalytically inactive FAK: a role for paxillin tyrosine phosphorylation. Mol Cell Biol 1997;17:6906–6914. [PubMed: 9372922]
49. Chen HY, Shen CH, Tsai YT, Lin FC, Huang YP, Chen RH. Brk activates rac1 and promotes cell migration and invasion by phosphorylating paxillin. Mol Cell Biol 2004;24:10558–10572. [PubMed: 15572663]
50. Thiery JP. Epithelial-mesenchymal transitions in tumour progression. Nat Rev Cancer 2002;2:442–454. [PubMed: 12189386]
51. Panetti TS. Tyrosine phosphorylation of paxillin, FAK, and p130CAS: effects on cell spreading and migration. Front Biosci 2002;7:d143–150. [PubMed: 11779709]
52. Kann ML, Soues S, Levilliers N, Fouquet JP. Glutamylated tubulin: diversity of expression and distribution of isoforms. Cell Motil Cytoskeleton 2003;55:14–25. [PubMed: 12673595]
53. Amar LS, Shabana AH, Oboeuf M, Martin N, Forest N. Involvement of desmoplakin phosphorylation in the regulation of desmosomes by protein kinase C, in HeLa cells. Cell Adhes Commun 1999;7:125–138. [PubMed: 10427965]
54. Amar LS, Shabana al HM, Oboeuf M, Martin N, Forest N. Desmosomes are regulated by protein kinase C in primary rat epithelial cells. Cell Adhes Commun 1998;5:1–12. [PubMed: 9638337]
55. Pasdar M, Li Z, Chan H. Desmosome assembly and disassembly are regulated by reversible protein phosphorylation in cultured epithelial cells. Cell Motil Cytoskeleton 1995;30:108–121. [PubMed: 7606804]
56. Toivola DM, Goldman RD, Garrod DR, Eriksson JE. Protein phosphatases maintain the organization and structural interactions of hepatic keratin intermediate filaments. J Cell Sci 1997;110(Pt 1):23–33. [PubMed: 9010781]
57. Toivola DM, Zhou Q, English LS, Omary MB. Type II keratins are phosphorylated on a unique motif during stress and mitosis in tissues and cultured cells. Mol Biol Cell 2002;13:1857–1870. [PubMed: 12058054]
58. Kitajima Y, Aoyama Y, Seishima M. Transmembrane signaling for adhesive regulation of desmosomes and hemidesmosomes, and for cell-cell detachment induced by pemphigus IgG in cultured keratinocytes: involvement of protein kinase C. J Invest Dermatol Symp Proc 1999;4:137–144.
59. Osada K, Seishima M, Kitajima Y. Pemphigus IgG activates and translocates protein kinase C from the cytosol to the particulate/cytoskeleton fractions in human keratinocytes. J Invest Dermatol 1997;108:482–487. [PubMed: 9077478]
60. Aoyama Y, Owada MK, Kitajima Y. A pathogenic autoantibody, pemphigus vulgaris-IgG, induces phosphorylation of desmoglein 3, and its dissociation from plakoglobin in cultured keratinocytes. Eur J Immunol 1999;29:2233–2240. [PubMed: 10427986]
61. Aoyama Y, Kitajima Y. Pemphigus vulgaris-IgG causes a rapid depletion of desmoglein 3 (Dsg3) from the triton X-100 soluble pools, leading to the formation of Dsg3-depleted desmosomes in a human squamous carcinoma cell line, DJM-1 cells. J Invest Dermatol 1999;112:67–71. [PubMed: 9886266]
62. Waschke J, Spindler V, Bruggeman P, Zillikens D, Schmidt G, Drenckhahn D. Inhibition of Rho A activity causes pemphigus skin blistering. J Cell Biol 2006;175:721–727. [PubMed: 17130286]
63. Fukata M, Nakagawa M, Kaibuchi K. Roles of Rho-family GTPases in cell polarisation and directional migration. Curr Opin Cell Biol 2003;15:590–597. [PubMed: 14519394]
64. Sander EE, ten Klooster JP, van Delft S, van der Kammen RA, Collard JG. Rac downregulates Rho activity: reciprocal balance between both GTPases determines cellular morphology and migratory behavior. J Cell Biol 1999;147:1009–1022. [PubMed: 10579721]
65. Nimnual AS, Taylor LJ, Bar-Sagi D. Redox-dependent downregulation of Rho by Rac. Nat Cell Biol 2003;5:236–241. [PubMed: 12598902]

66. Nobes CD, Hall A. Rho GTPases control polarity, protrusion, and adhesion during cell movement. J Cell Biol 1999;144:1235–1244. [PubMed: 10087266]

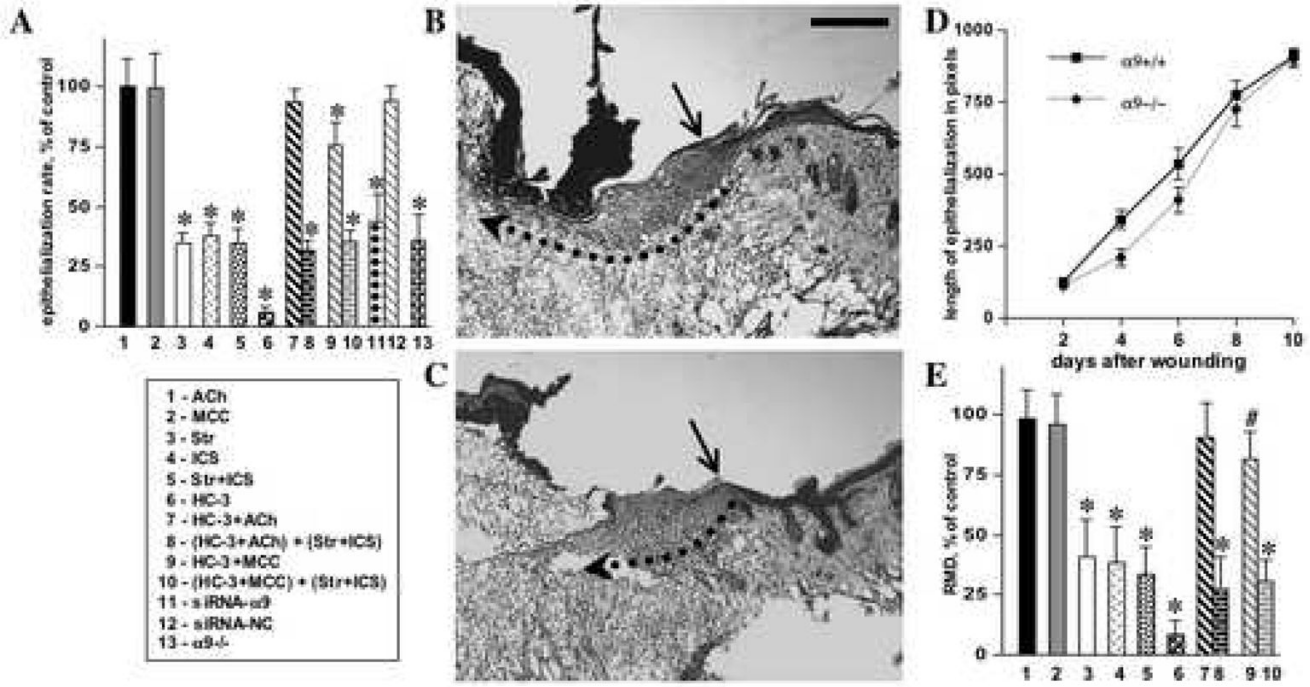

Figure 1. Role of α9 AChR in wound healing *in vitro* and *in vivo*

A. Effects on wound epithelialization *in vitro*. The migration of KCs was measured using the scratch assay. The experimental conditions tested are shown in the box. The following concentrations were used: ACh—1 mM, MCC—0.1 mM, Str—0.1 μM, ICS—0.1 μM, and HC-3—20 μM. Before induction of migration, some KCs were transfected with siRNA directly in the scratch assay plates. The results are expressed as % of control, which in all experiments with human KCs represented the values obtained in untreated cultures, and in experiments with α9−/− murine KCs—the values obtained with α9+/+ cells. Asterisks indicate $p<0.05$, the rest are $p>0.05$.

B, C. The representative images of wound tissue of wild type (**B**) and α9 knockout (**C**) mice harvested on the 4th day post wounding. The edge of the full thickness wound extending from the epidermis down to the dermis is depicted by an arrow. The direction of forward movement of the epithelial tongue from the excision site is indicated with a dotted line with an arrowhead. Bar = 100 μm.

D. Rate of epithelialization of skin wounds in α9+/+ *vs*. α9−/− littermates. The rate of epithelialization of square excisional wounds inflicted in the back skin of wild type and α9 knockout mice was determined 2, 4, 6, 8 and 10 d after wounding, using the morphometric analysis described in Materials and Methods. The data are means ± SD of the length of epithelialization tongue computed in at least three α9−/− mice, compared to that determined in their wild type α9+/+ littermates. The differences are significant ($p<0.05$) on the 4th and 6th days post wounding.

E. Effects on keratinocyte outgrowth from the megacolony. The KCs were loaded in AGKOS plates, allowed to form a confluent megacolony after which the migration was induced by co-stimulation with EGF and either ACh or MCC in the presence or absence of antagonists at the concentrations indicated in the panel A. Results are expressed as % of control of random migration distances (**RMD**) measured in control cultures treated with KGM containing EGF without other additions. Asterisks indicate $p<0.05$, and pound sign indicates $p=0.05$, the rest are $p>0.05$.

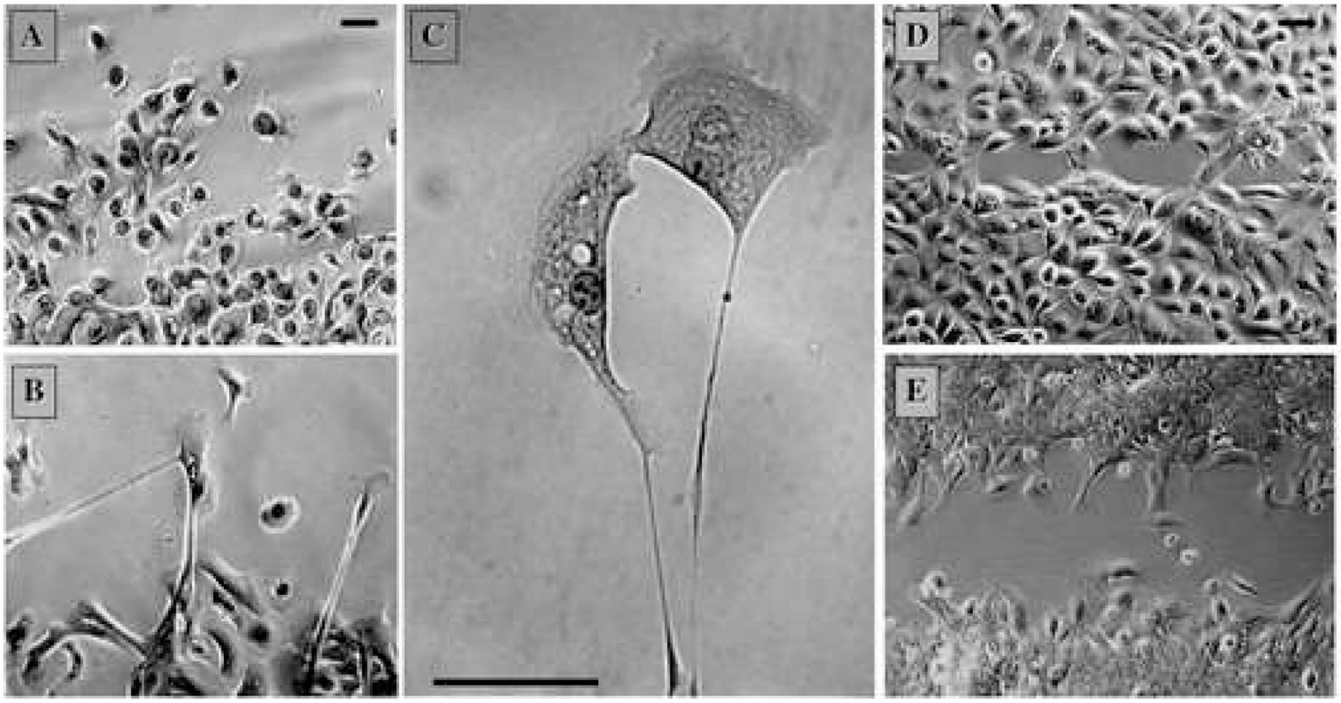

Figure 2. Blockade of α9 AChR alters migratory phenotype of KCs

KCs at the leading edge of control megacolony in an AGKOS plate exhibited normal, letter "D"-like migratory phenotype produced due to extension of the lamellipodium and retraction of the trailing edge (**A**). In contrast, KCs treated with a mixture of α9 antagonists Str and ICS, 0.1 μM each, exhibited altered morphology (**B, C**). Although the cells at the leading edge elongated, acquired a bipolar shape, extended lamellipodium and moved forward, many of them remained anchored to the culture substrate with stretched cytoplasmic processes being unable to retract the uropod. Similar elongated morphology was observed in KCs transfected with siRNA-α9 at the leading edge of the re-epithelializing monolayers in the scratch assay plates (**D, E**). Note: 24 h after scratching, the gap between wound edges was almost completely closed in the monolayers comprised by KCs transfected with siRNA-NC (**D**) but not siRNA-α9 (**E**). Bars = 50 μm.

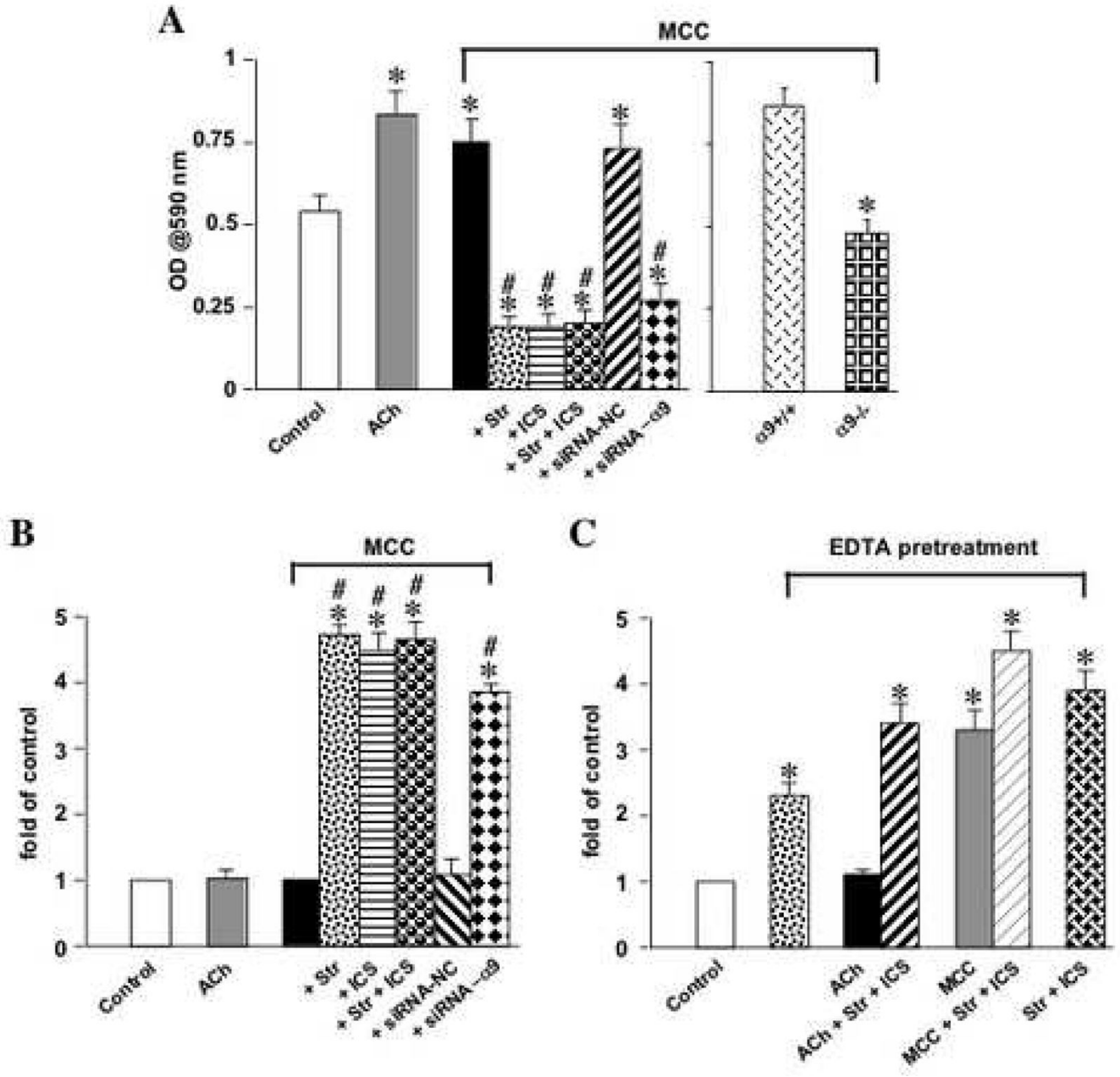

Figure 3. Regulation of keratinocyte cell-matrix and cell-cell adhesion through α9 AChR

A. Effects on cell-matrix attachment of suspended KCs. The OD values were measured at 590 nm after a 1 h incubation of suspension of normal or siRNA-transfected human KCs or α9+/+ *vs.* α9−/− murine KCs in KGM containing 1 mM ACh, or 0.1 mM MCC, alone or in combination with Str, 0.1 μM and/or ICS, 0.1 μM. Asterisks indicate $p<0.05$ compared to intact control cells and pound sign indicates $p<0.05$ compared to KCs treated with MCC alone.

B. Effects on cell-cell attachment in confluent monolayer. The PC values were measured 1 h after confluent monolayers of normal or siRNA transfected human KCs in membrane-bottomed chamber inserts were exposed to the cholinergic compounds at the doses described in panel A. The results are expressed as fold of control values determined in intact cultures. Asterisks indicate $p<0.05$ compared to control cells and pound sign indicates $p<0.05$ compared to KCs treated with MCC alone.

C. Effects on cell-cell attachment in dissociated cultures. The PC values were measured 1 h after the monolayers of normal human KCs were dissociated with 0.53 mM EDTA for 30 sec and then exposed to test cholinergic compounds shown in the graph in the same concentrations as in panels A and B. Asterisks indicate $p<0.05$ compared to intact control cells.

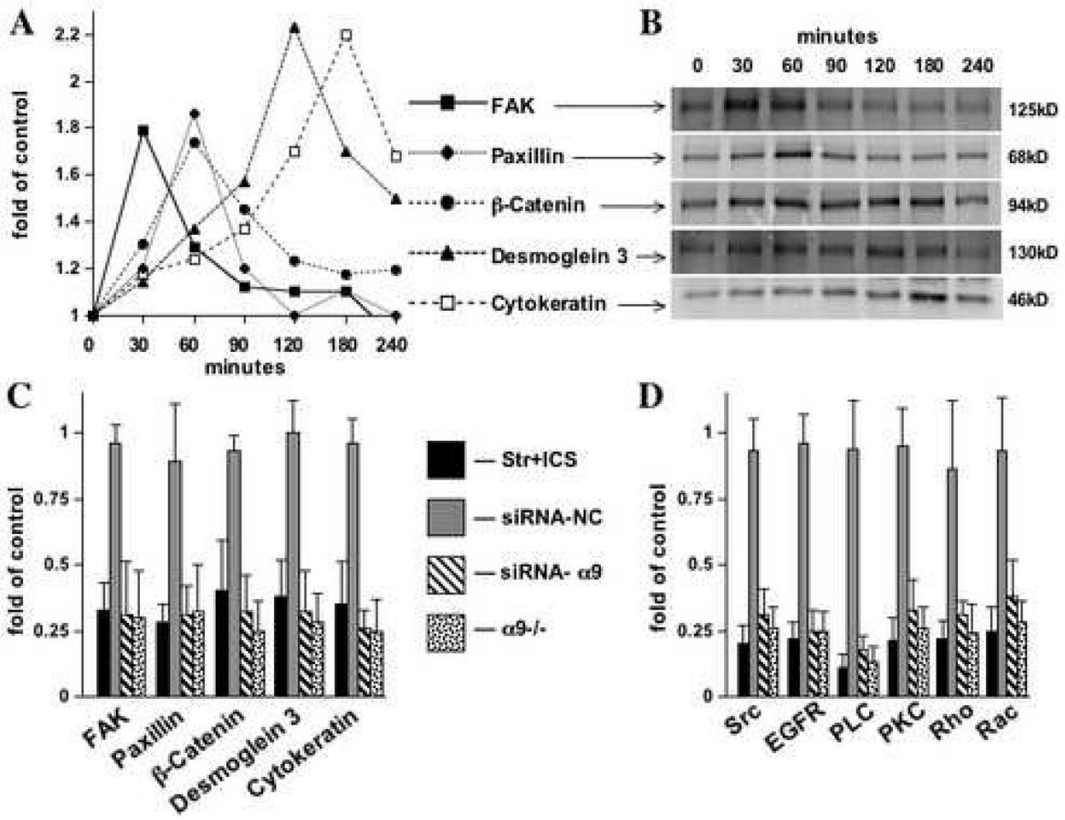

Figure 4. Role of α9 AChR in regulation of phosphorylation of adhesion and cytoskeletal proteins in KCs

A. Time-course analysis of the phosphorylation status of keratinocyte proteins subsequent to α9 AChR activation. The confluent keratinocyte monolayers established in 6-well plates were incubation for 6 h at 1.2 mM Ca^{2+} in KGM, starved of EGF for 18 h, and then fed with KGM containing 10 ng/ml EGF and 0.1 mM MCC. After incubation for the time periods shown in the graph, the cells were lysed and used to measure the levels of phosphorylation as detailed in Materials and Methods. Results are expressed as mean fold of control values measured in the monolayers that did not receive MCC.

B. The representative images of the phosphorylated adhesion molecules and cytoskeletal proteins from the time-course experiments reported in panel A. The images show typical bands that appeared at each time point at the expected molecular weights shown to the right of gels.

C. Inhibition of α9 AChR signaling reduced phosphorylation of adhesion and cytoskeletal proteins. The monolayers of human KCs were stimulated as described in the panel A and analyzed at the point of the highest phosphorylation of each molecule, i.e., at the 30^{th} min for FAK, 60^{th} min for paxillin and β-catenin, 120^{th} min for desmoglein 3 and 180^{h} min for cytokeratins. The inhibition of α9 AChR signaling was achieved due to treatment with the pharmacologic inhibitors Str, 0.1 μM plus ICS, 0.1 μM, transfection with siRNA-α9 or α9 null mutation. The results are expressed as fold of control. The values determined in cultures that did not receive antagonists served as control in experiments with the Str+ICS and siRNA transfection, and α9+/+ murine KCs served as control for α9−/− cells. In all experiments, except for transfection with siRNA-NC, the results significantly ($p<0.05$) differ from control values.

D. Inhibition of α9 AChR signaling inhibits activities of effector molecules. The monolayers were stimulated exactly as described in panel A and α9 AChR signaling was inhibited exactly as described in the panel B. The results are expressed as fold of control of the activity of each effector molecule determined at the time point of its highest activity after activation of α9

AChR shown in Fig. 5, i.e., at the 15th min for Src, 30th min for EGFR, 60th min for PLC, Rho and Rac, and 90th min for PKC. In all experiments, except for transfection with siRNA-NC, the results significantly ($p<0.05$) differ from control values.

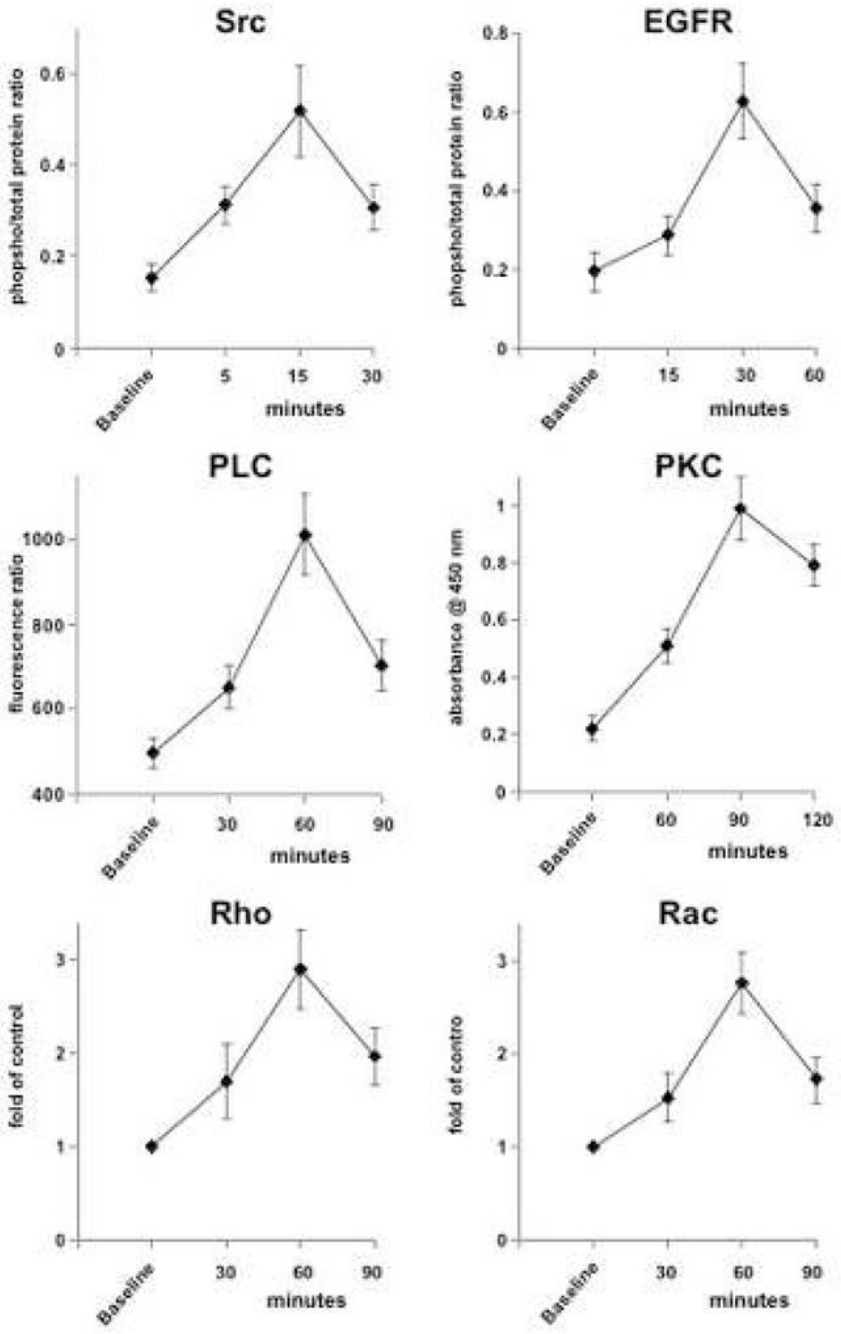

Figure 5.

Time-course analysis of the activities of Src, EGFR kinase, PKC, PLC, Rho and Rac following activation of α9 AChR. The α9 AChR in normal human KCs was activated as described in the panel A of Fig 4, and the activities of effector molecules were measured in accordance to the protocols provided by the manufacturers of the activity assay kits described in Materials and Methods. The data are mean ± SD of the results obtained in three independent experiments.

Table 1

Effect of α9 AChR inhibition on colony scattering induced by HGF/SF

Treatment condition[1]	Extent of scattering[2]
Stimulation with HGF/SF alone	+++[3]
Stimulation with HGF/SF plus:	
ACh, 1 mM	+++
MCC, 0.1 mM	+++
Str, 0.1 μM	++
ICS, 0.1 μM	++
Str + ICS	+
HC-3, 20 μM	—
HC-3 + ACh	+++
HC-3 + MCC	+++
HC-3 + ACh + Str + ICS	+
HC-3 + MCC + Str + ICS	—
siRNA-α9	—
siRNA-NC	—

[1] — There was no scattering in the absence of HGF/SF.

[2] — No visible colony dispersion.

[3] — Legend: + singe cell break away from the colony (<10% dissociated cells); ++ partial colony dissociation (10–75%); +++ complete dissociation (>75% dissociated cells).